Photonic simulation of system-environment interaction: Non-Markovian processes and dynamical decoupling

Chang-Ling Zou, Xiang-Dong Chen, Xiao Xiong, Fang-Wen Sun,* Xu-Bo Zou, Zheng-Fu Han, and Guang-Can Guo
Key Lab of Quantum Information, University of Science and Technology of China, Hefei 230026, China
(Received 18 March 2013; published 2 December 2013)

The system-environment interaction is simulated by light propagating in coupled photonic waveguides. The profile of the electromagnetic field provides intuitive physical insight to study the Markovian and non-Markovian dynamics. The transition from non-Markovian to Markovian process is demonstrated by increasing the size of the environment, as the energy evolution changes from oscillation to exponential decay and the revival period increases. Moreover, the dynamical decoupling with a sequence of phase modulations is introduced to such a photonic system to form a band structure in the time dimension, where the energy dissipation can be significantly accelerated or inhibited. It opens the possibility to tune the dissipation in a photonic system, similar to the dynamic decoupling of spins.

DOI: 10.1103/PhysRevA.88.063806 PACS number(s): 42.50.Ct, 05.45.Mt, 42.25.−p, 42.60.Da

I. INTRODUCTION

Quantum systems always inevitably interact with environments, which can change the quantum states and lead to energy dissipation and decoherence of the systems [1,2]. For a deep understanding and broad applications of quantum effects, great efforts have been made to study the system-environment (SE) interaction. Lots of interesting phenomena of open quantum systems have been studied, such as the Zeno and anti-Zeno effects [3,4], and transition between quantum Markovian and non-Markovian processes [5,6]. Advanced quantum techniques related to the environment have been developed and remarkable progresses have been achieved in experiments, such as the dissipation engineering to prepare and control quantum states with the help of the environment [7–10], and dynamical decoupling to preserve the quantum coherence from the environmental noise [11–13]. However, it is still difficult to fully control various environments, which highly limits the understanding, control, and application of this SE interaction.

Recently, increasing theoretical and experimental efforts were focused on quantum simulations [14–16], which was inspired by Feynman's seminal idea [17]. Various complex and important physical phenomena can be studied by quantum simulators with high efficiency, such as quantum decoherence [18], many-body physics, the mechanism of superconducting, and general relativity [15]. Such quantum simulations can provide different views to study subtle physical processes and reveal new phenomena. And more importantly, people can also learn new ideas from the complementary interdiscipline and exploit quantum physics to design new devices for quantum technology and practical applications. For example, the photonic simulation of electron spins can be used for topological protected delay [19], and the simulation of adiabatic passage in a waveguide can be applied to a high-efficiency optical coupler [20,21] and polarization rotator [22].

In this paper, we simulate the quantum open system by photons in an integrated photonic chip. The underlying physics of the SE interaction is revealed intuitively by simply observing the electromagnetic field transmission, spreading in the environment, reflection at the boundary of the environment, and reflowing back to the system. Non-Markovian and Markovian processes of this photonic system are studied by varying the size of the environment. Due to the memory effect of a finite environment (the energy in the environment is reflected back by the boundary of environment), the dynamics of the system is non-Markovian which shows nonexponential decay and revival, whereas for the environment with infinite size, the system shows Markovian exponential decay. Furthermore, the system decay can be controlled by dynamical decoupling with external phase modulations, where the dissipation to the environment can be accelerated or inhibited. Our study provides an intuitive understanding of the SE interaction, and the results can also be used to analyze and reduce the leakage losses of photonic structures.

II. MODEL

As illustrated by the inset of Fig. 1(a), the proposed photonic simulation of the SE interaction is composed of two separated waveguides. Light is loaded at *system* waveguide (SW) and travels along it (z axis). The system is open because its energy can dissipate to the nearby *environment* waveguide (EW). The light in a single isolated waveguide can be described by the Helmholtz equation as [23]

$$\nabla^2\psi(\vec{r}) + V(\vec{r})\psi(\vec{r}) = E\psi(\vec{r}), \tag{1}$$

where $V(\vec{r}) = [\varepsilon(\vec{r}) - 1]k^2$ and $E = -k^2$, with dielectric relative permittivity $\varepsilon(\vec{r})$ and wave number $k = 2\pi/\lambda$. The waveguides are uniform along the z axis. Therefore, the ith propagating eigenmode's wave function is expressed as $\psi_i(\vec{r}) = \varphi_i(x,y)e^{-in_i kz}$, where $\varphi_i(x,y)$ is the field distribution at the cross section of a waveguide, and n_i is the effective mode index which can be solved from the characteristic equation (Appendix A). For coupled SW and EW, we can decompose any field distribution perturbatively as

$$\psi(\vec{r}) = \sum_{i=1}^{N_s} c_i^s(z)\psi_i^s(\vec{r}) + \sum_{j=1}^{N_e} c_j^e(z)\psi_j^e(\vec{r}), \tag{2}$$

*fwsun@ustc.edu.cn

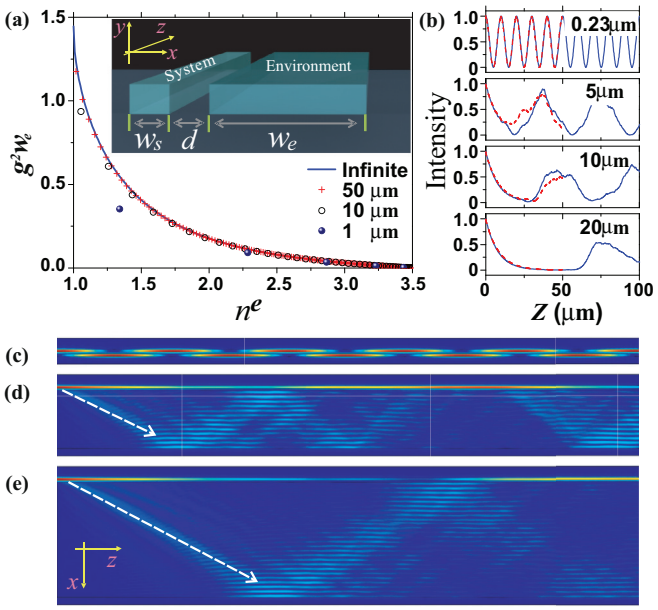

FIG. 1. (Color online) (a) The normalized coupling strength $g^2 w_e$ between system and environment against effect mode index n^e for different environment size w_e. Inset: schematic illustration of the coupled photonic waveguides simulating the SE interaction. (b) Typical dynamics of energy in SW against the interaction length z for different w_e, where solid and dashed lines are analytical and numerical results, respectively. (c)–(e) False-color profiles of electric field intensity in SW and EW, with light loaded in the SW at $z = 0$ and wavelength $\lambda = 1550$ nm, $d = 0.15$ μm and $w_e = 0.23$, 5, and 10 μm, respectively.

where s and e denote SW and EW, respectively; $N_{s(e)}$ is the number of modes in the SW (EW); and $\psi^{s(e)}_{i(j)}(\vec{r})$ are eigenmodes of SW (EW) with the corresponding coefficients $c^{s(e)}_{i(j)}(z)$. Substituting $V(\vec{r}) = V^s(\vec{r}) + V^e(\vec{r})$ and $\psi(\vec{r})$ into Eq. (1), we can obtain the dynamics of the modes in each waveguide approximately as (Appendix B)

$$i\frac{\partial c_i^{s(e)}}{\partial z} = \sum_{l=1}^{N_{s(e)}} m_{il}^{s(e)} e^{i(n_i^{s(e)} - n_l^{s(e)})kz} c_l^{s(e)} + \sum_{j=1}^{N_{e(s)}} g_{ij}^{s(e)} e^{i(n_i^{s(e)} - n_j^{e(s)})kz} c_j^{e(s)}, \quad (3)$$

where coefficients $m_{il}^{s(e)} = \frac{\iint (\varphi_i^{s(e)})^* V^{s(e)} \varphi_l^{s(e)} dxdy}{2n_i^{s(e)}k}$ and $g_{ij}^{s(e)} = \frac{\iint (\varphi_i^{s(e)})^* V^{s(e)} \varphi_j^{e(s)} dxdy}{2n_i^{s(e)}k}$, with all wave functions normalized by $\iint |\varphi_i^{s(e)}|^2 dxdy = 1$.

Here, we consider a thin single-mode SW ($N_s = 1$) interacting with multimode EW, with $N_e \geqslant 1$ depending on its width w_e. Denoting the system and environment fields by $a = c_1^s e^{-in_1^s kz}$ and $b_j = \sqrt{g_{1j}^s / g_{1j}^e}\, c_j^e e^{-in_j^e kz}$, and replacing the space coordinate z by time t, we can obtain the Hamiltonian which governs the dynamics of this photonic simulation of the SE interaction as ($\hbar = 1$)

$$H = \beta_0 a^\dagger a + \sum_j \beta_j b_j^\dagger b_j + \sum_j g_j (a^\dagger b_j + a b_j^\dagger), \quad (4)$$

where $\beta_0 = (n_1^s + m_{11}^s)k = n_0 k$ and $\beta_j = (n_j^e + m_{jj}^e)k = n_j k$ are propagation constants, and $g_j = \sqrt{g_{1j}^s g_{1j}^e}$ is the coupling coefficient. Since the direct coupling between environment modes is much smaller than other terms, $m_{i,j}^e$ $(i \neq j)$ is neglected in the following studies.

III. NON-MARKOVIAN AND MARKOVIAN PROCESSES

The Hamiltonian of Eq. (4) resembles an open system in which a harmonic oscillator (a) couples to a collection of oscillators in the environment (b_j). Here, both the coupling coefficients and the size of the environment can be well controlled in the coupling waveguides, which is very promising to simulate the SE interaction. With two-dimensional approximation, β_j and g_j can be solved analytically (Appendix C). In the following, we studied the model with photonic waveguides made of silicon ($n_d = 3.5$), which have been extensively studied in practical experiments. The working wavelength (λ) is 1550 nm, and the width of SW is fixed to $w_s = 0.23$ μm in the single-mode regime.

The normalized coupling strength ($g^2 w_e$) between system and environment against mode index $n^e = \beta_j / k$ is shown in Fig. 1(a). The continuum of the finite size environment is quantized to discrete modes, whose density and number N_e increases with w_e. When w_e approaches infinity, $g^2 w_e$ converges to a line described by an analytical formula [see Eq. (D12) in Appendix D]. With these parameters, the dynamics of SE interaction can be solved according to Eq. (4). In Fig. 1(b), the evolutions of energy in the SW against z for different w_e are calculated, with light loaded in the SW at $z = 0$. For comparison, the fields in the SW are also simulated by solving the Maxwell equations numerically with the finite element method. The results of our SE interaction model agree very well with numerical results, with small discrepancies originating from the slowly varying and weak-coupling approximations used in our analytical expressions. For small environment ($w_e = 0.23$ and 5 μm), the dynamics of energy in the SW shows periodic oscillation. When the environment size increases, the energy in the SW shows exponential decay at first and revives after a distance.

A direct view of the dynamics of the coupled SE can be obtained from Figs. 1(c)–1(e). When w_e is comparable with λ, only a few modes in the EW can be involved to interact with the system. As a result, the coherent coupling leads to a sinusoidal oscillation of energy in the SW [Fig. 1(c)]. For larger w_e, more modes in the EW interact with the SW, giving rise to complex dynamics. The cooperation of environmental modes shows a classical ray trajectory with spreading, as indicated by the dashed line in Fig. 1(d), with an incident angle $\chi = \arcsin(\beta_0 / n_d k)$ with respect to the x axis. When $w_e \geqslant 10$ μm, the energy in the SW exponentially decays with z and can almost completely leak into the environment [Fig. 1(e)]. After a certain distance, the leakage will be reflected and reflow back into the SW, causing the revival.

Some important properties of SE interaction and intuitive understanding of the underlying physics can be easily obtained from those figures. The formal solution to the system dynamics

is derived in the interaction picture

$$H_I(z) = \sum_j \hbar g_j (a^\dagger b_j e^{i(\beta_0-\beta_j)z} + a b_j^\dagger e^{-i(\beta_0-\beta_j)z}). \quad (5)$$

By employing the formal solution

$$b_j(z) = -i g_j \int_0^z a(\tau) e^{-i(\beta_0-\beta_j)\tau} d\tau, \quad (6)$$

the dynamics of system reads

$$\frac{\partial}{\partial z} a(z) = -\int_0^z a(\tau) K(\tau - z) d\tau, \quad (7)$$

with the memory kernel function $K(\tau) = \sum_j g_j^2 e^{-i(\beta_0-\beta_j)\tau}$ [1]. For small w_e, the beating of multiple modes in the EW gives rise to the oscillation behavior of $K(\tau)$ [Fig. 2(a)]. The nonzero memory effect leads to non-Markovian dynamics with nonexponential decay and the revival phenomenon in the SW, as shown in Fig. 2(b). Since the period of $K(\tau)$ is determined by the environmental mode density $\rho(n) \approx \frac{k w_e}{\pi} \frac{n}{\sqrt{n_d^2 - n^2}}$ (Appendix D), the non-Markovian revival period linearly depends on w_e, which can be observed in Fig. 2(b) where the revival period (R) is larger for larger w_e. We can also deduce the revival period $R = 2w_e \tan\chi + R_0$ with intuitive understanding of revival as a beam reflection at the boundary of the environment. The revival period extracted from the dynamics of the system is well fitted by this formula, as shown in Fig. 2(c). The constant R_0 comes from an extra distance required for tunneling [24] and Goos-Hänchen shift [25] of light reflection at the environmental boundary.

Figure 2(a) shows that the oscillation of $K(\tau)$ is suppressed for very large environment size. As a great many environmental modes are involved when $w_e \to \infty$, the memory kernel function can be approximately written in the form of integration,

$$K(\tau) = \int g^2(n) e^{-i(\beta_0 - nk)\tau} \rho(n) dn, \quad (8)$$

where the coupling strength $g(n)$ is a function of mode index n [Fig. 1(a)]. Then, $K(\tau) \approx J(n_0)\delta(\tau)$, where $\delta(\tau)$ is the Dirac δ function, $n_0 = \beta_0/k$, and

$$J(n) = g^2(n) w_e \frac{n}{\sqrt{n_d^2 - n^2}} \quad (9)$$

is the spectrum density function of the reservoir. Substituting the memory function $K(\tau) = J(n_0)\delta(\tau)$ into Eq. (7), we obtain that the energy in the SW decays exponentially as $a(z) = e^{-z/2L}$, where the decay length is (Appendix D)

$$L \approx L_0 e^{2\sqrt{n_0^2 - 1} k d}, \quad (10)$$

with

$$L_0 = \frac{1}{k} \frac{n_0 (n_d^2 - 1)^2 (k w_s + 2/\sqrt{n_0^2 - 1})}{8(n_0^2 - 1)(n_d^2 - n_0^2)^{3/2}}. \quad (11)$$

In Fig. 2(d), the analytical decay length is compared to the results extracted from the dynamics of the system with logarithmic fitting. Our prediction is consistent with the data. The slight discrepancy is due to nonflat noise spectrum density. It is surprising that the formula of L in the continuum limit works for small w_e, as shown in the inset of Fig. 2(d). The oscillation is due to the variation of the mode index of discrete modes in a finite environment.

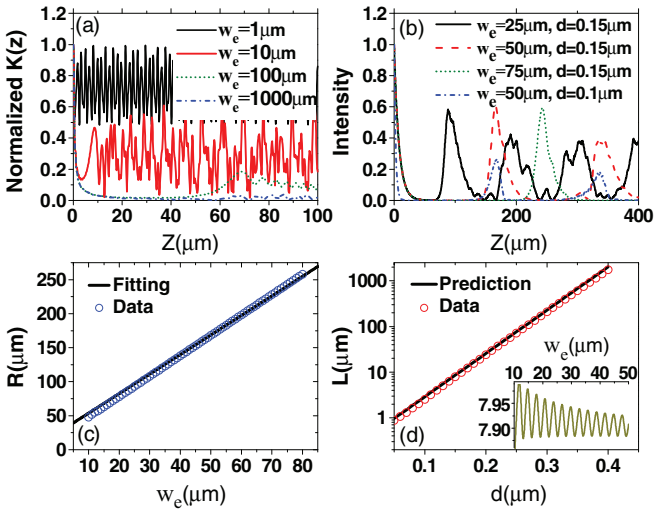

FIG. 2. (Color online) (a) The memory kernel function $K(z)$ for different environment sizes, with $d = 0.15$ μm. (b) The dynamics of energy in SW for different w_e and d. (c) The revival period R against w_e, with $d = 0.15$ μm. The circles are obtained from the SE interaction model, which is fitted by the beam reflection formula (solid line). (d) The decay length of energy in SW against d, where the circles are obtained from the SE interaction model and the solid line is from the analytical formula for $w_e = \infty$. Inset: the decay length against w_e.

IV. DYNAMICAL DECOUPLING

It is well known that external modulation to an open quantum system can modify the energy decay and decoherence, and the so-called dynamical decoupling technique has been widely adopted to keep the coherence of electron spins [11–13]. Similarly, for the photonic simulation of SE interaction, a dynamical modulation of the SW can also alter the energy decay. Here, a sequence of modulations (N) with equal interval is applied to the SW, where each modulation corresponds to an abrupt change of phase ϕ. Figure 3(a) shows the evolution of the SW changing with different modulations. The dissipation of the system can be enhanced or inhibited significantly depending on ϕ and N. Figures 3(c) and 3(d) show the energy in the SW at $z = 50$ μm against the modulation phase ϕ with different w_e and N.

There is an intuitive way to understand the modified decay: the modulations add extra phase to the propagating light, which is equivalent to the increase or decrease of the effective index $\tilde{n}$, as the phase of a propagating photon is proportional to $\tilde{n}$. As shown in Fig. 3(b), the spectrum of the dynamics of the system is shifted by the modulations. According to the spectrum density of reservoir [Fig. 1(a)], the shifting of $\tilde{n}$ corresponds to changing of the SE coupling strength; thus, it gives rise to acceleration or deceleration of energy dissipation in the SW. When $\tilde{n}$ is larger than the cutoff index n_d, the dissipation of energy in the SW to the EW is forbidden. From another point of view, the waveguide with periodic modulations is

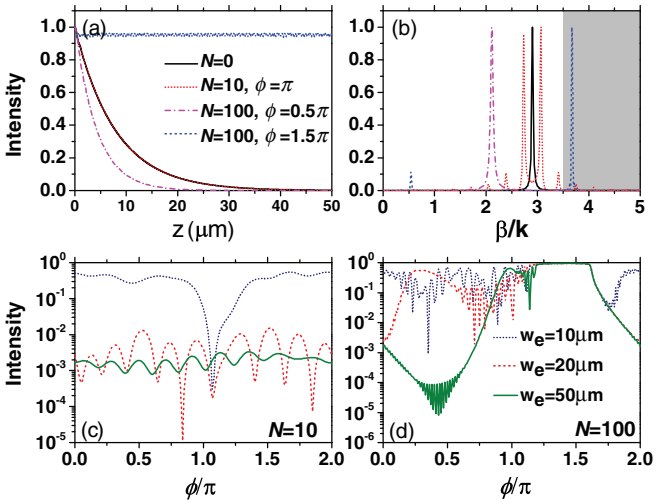

FIG. 3. (Color online) (a) The evolution of energy in the SW and (b) corresponding spectrum when a sequence of N modulations of phase ϕ is applied to the SW, with $w_e = 50$ μm and $d = 0.15$ μm. (c), (d) Energy in the SW at $z = 50$ μm against ϕ for different w_e and N, with $d = 0.15$ μm.

similar to a photonic crystal or grating structure, which will induce a band structure to light. By this means, noise in an environment can be prevented from propagating in the system. These provide physical insight to the dynamical decoupling in the time dimension where a sequence of modulations in the time axis is applied: the effective frequency of the system shifts to a higher value than the cutoff frequency of the bath. Or, we can imagine a crystal or band structure in the time dimension, where only a signal with certain frequencies can enter and be kept in the system while most of the broadband noise in the environment is blocked.

One way to realize such a phase modulation sequence is shown in Fig. 4(a), with whispering gallery mode (WGM) microdisks coupling to the SW [26]. The microdisk with radius $r = 1$ μm has an intrinsic quality factor higher than

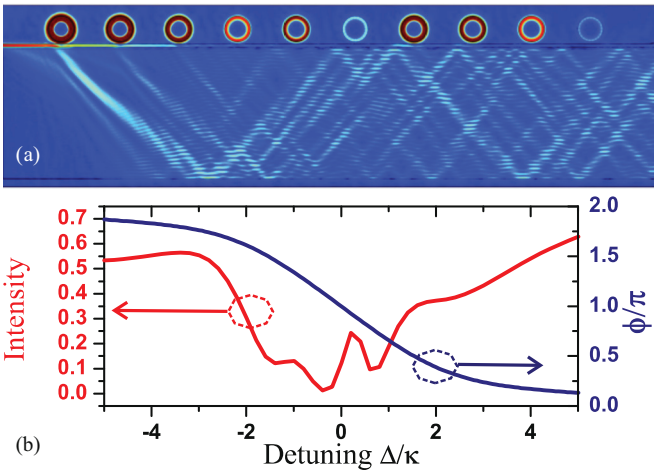

FIG. 4. (Color online) (a) The fields of system and environment waveguides when microdisks are added to the waveguide to induce a phase modulation. (b) The dynamics against the detuning of input light to the whispering gallery modes.

1×10^6. When the microdisk is placed close to the SW with a gap (0.15 μm), the loaded quality factor of the WGM is only about 2000. That means that the WGM works in the strong overcoupling regime with $\kappa_e \gg \kappa_i$, where $\kappa_{i(e)}$ is the intrinsic (external) loss. When the light in the system passes the overcoupled WGM resonator, the change of transmitted light is

$$T(\Delta) = -\frac{1 - i\Delta/(\kappa_e - \kappa_i)}{1 + i\Delta/(\kappa_e + \kappa_i)} \approx -\frac{1 - i\Delta/\kappa_e}{1 + i\Delta/\kappa_e}, \qquad (12)$$

where Δ is the frequency detuning to the resonance. As $|T(\Delta)| \approx 1$, the system acquires a modulation of phase $\phi(\Delta) = \arg[T(\Delta)]$. Numerical simulation of the dynamical decoupling with $N = 10$ for $w_e = 10$ μm is performed. Comparing the mode profile of Fig. 4(a) with Fig. 1(e), the evolutions are significantly changed by modulations. In Fig. 4(b), a strong modification of the transmitted energy in the SW at $z = 50$ μm is shown around the resonance with $\phi \approx \pi$, which is consistent with the prediction in Fig. 3(c).

V. CONCLUSION

The Markovian and non-Markovian processes and dynamic decoupling of open quantum systems are studied in a photonic simulation of SE interaction. Intuitive physical insight and understanding of these phenomena can be gained from the direct view of the electromagnetic field profiles. Our study also opens the possibility to tune the dissipation in a photonic system, similar to the dynamic decoupling of spins. It also bridges the well-studied electronic and optical systems, which may bring new ideas from each other.

ACKNOWLEDGMENTS

This work was supported by the 973 Programs (No. 2011CB921200 and No. 2011CBA00200), the National Natural Science Foundation of China (NSFC) (Grant No. 11004184), and the Knowledge Innovation Project of the Chinese Academy of Sciences (CAS).

APPENDIX A: EIDENMODES IN WAVEGUIDE

For a single waveguide with width w and refractive index n_d, we have the eigenmode wave function in the form

$$\psi_i(\vec{r}) = \varphi_i(x,y)e^{-in_i kz}, \qquad (A1)$$

where $\varphi_i(x,y)$ is the field distribution at the cross section of a waveguide, and n_i is the effective mode index. In a two-dimensional waveguide (x-z plane), the mode wave function $\varphi_i(x)$ and n_i can be solved analytically. For the even symmetry mode, the wave function at the cross section of the waveguide has the form

$$\varphi(x) = \begin{cases} \cos\frac{\alpha w}{2} e^{\gamma(x+w/2)}, & x < -\frac{w}{2} \\ \cos\alpha x, & -\frac{w}{2} < x < \frac{w}{2} \\ \cos\frac{\alpha w}{2} e^{-\gamma(x-w/2)}, & x > \frac{w}{2}, \end{cases} \qquad (A2)$$

and for the odd symmetry mode,

$$\varphi(x) = \begin{cases} -\sin\frac{\alpha w}{2} e^{\gamma(x+w/2)}, & x < -\frac{w}{2} \\ \sin\alpha x, & -\frac{w}{2} < x < \frac{w}{2} \\ \sin\frac{\alpha w}{2} e^{-\gamma(x-w/2)}, & x > \frac{w}{2}, \end{cases} \tag{A3}$$

where $\alpha = k\sqrt{n_d^2 - n_{\text{eff}}^2}$, $\gamma = k\sqrt{n_{\text{eff}}^2 - 1}$. Here, each wave function is normalized by the maximum field amplitude. According to the boundary condition that $\partial\varphi(x)/\partial x$ is continuous for transverse magnetic modes, we can obtain the characteristic equations for the even symmetry mode,

$$\tan\frac{\alpha w}{2} = \frac{\gamma}{\alpha}, \tag{A4}$$

and for the odd symmetry mode,

$$\tan\frac{\alpha w}{2} = -\frac{\alpha}{\gamma}. \tag{A5}$$

All eigenmodes can be solved by the characteristic equations, and the number of modes depends on the waveguide width w.

APPENDIX B: COUPLED MODE THEORY

For coupled waveguides, the Helmholtz equation becomes

$$\nabla^2\psi(\vec{r}) + [V^s(\vec{r}) + V^e(\vec{r})]\psi(\vec{r}) = E\psi(\vec{r}). \tag{B1}$$

Substituting the perturbative expansion of the wave function [Eq. (2)] to Eq. (B1), we obtain

$$\begin{aligned} &\sum_i c_i^s(z)\left\{\nabla^2\psi_i^s(\vec{r}) + [V^s(\vec{r}) + V^e(\vec{r}) - E]\psi_i^s(\vec{r})\right\} \\ &+ \sum_j c_j^e(z)\left\{\nabla^2\psi_j^e(\vec{r}) + [V^s(\vec{r}) + V^e(\vec{r}) - E]\psi_j^e(\vec{r})\right\} \\ &+ \sum_i 2\frac{\partial}{\partial z}\psi_i^s(\vec{r})\frac{\partial}{\partial z}c_i^s(z) + \sum_j 2\frac{\partial}{\partial z}\psi_j^e(\vec{r})\frac{\partial}{\partial z}c_j^e(z) \\ &+ \sum_i \psi_i^s(\vec{r})\frac{\partial^2}{\partial z^2}c_i^s(z) + \sum_j \psi_j^e(\vec{r})\frac{\partial^2}{\partial z^2}c_j^e(z) = 0. \end{aligned} \tag{B2}$$

Under the slowly varying approximation

$$\frac{\partial^2}{\partial z^2}c_i^{s(e)}(z) \ll \frac{\partial^2}{\partial z^2}\psi_i^{s(e)}(\vec{r}), \tag{B3}$$

the last two terms can be neglected. In addition, the wave function in the SW (EW) satisfies the Helmholtz equation

$$\nabla^2\psi_i^{s(e)}(\vec{r}) = [E - V^{s(e)}(\vec{r})]\psi_i^s(\vec{r}). \tag{B4}$$

Thus, Eq. (B2) is simplified as

$$\begin{aligned} &\sum_i c_i^s(z)V^e(\vec{r})\psi_i^s(\vec{r}) + \sum_j c_j^e(z)V^s(\vec{r})\psi_j^e(\vec{r}) \\ &+ \sum_i 2\frac{\partial}{\partial z}\psi_i^s(\vec{r})\frac{\partial}{\partial z}c_i^s(z) + \sum_j 2\frac{\partial}{\partial z}\psi_j^e(\vec{r})\frac{\partial}{\partial z}c_j^e(z) = 0 \end{aligned} \tag{B5}$$

Multiplying Eq. (B5) by $(\psi_i^s)^*$ and integrating the result over the cross section of the waveguide, we obtain

$$\begin{aligned} &2in_i^s k\frac{\partial}{\partial z}c_i^s(z)\iint |\varphi_i^s|^2 dxdy \\ &\approx \sum_l c_l^s(z)e^{i(n_i^s - n_l^s)kz}\iint (\varphi_i^s)^* V^e(\vec{r})\varphi_l^s dxdy \\ &\quad + \sum_j c_j^e(z)e^{i(n_i^s - n_j^e)kz}\iint (\varphi_i^s)^* V^s(\vec{r})\varphi_j^e dxdy. \end{aligned} \tag{B6}$$

Here, the orthogonal relation

$$\iint (\psi_i^{s(e)})^*\psi_j^{s(e)} dxdy = 0 \quad \text{if} \quad i \neq j, \tag{B7}$$

and the approximation

$$\iint (\psi_i^{e(s)})^*\psi_j^{s(e)} dxdy \approx 0 \tag{B8}$$

are employed.

Finally, we arrive at the simplified coupled mode equations [Eq. (3)].

APPENDIX C: ANALYTICAL RESULTS

1. Wave-function normalization

In the expressions of coupling coefficients, there is an integration term $\iint |\varphi_i|^2 dxdy$ in the denominator as a normalization of wave functions. The integration corresponds to the total energy of the modes. From the symmetry, we have

$$\begin{aligned} \frac{1}{2}\int |\varphi|^2 dx &= \left[f\left(\frac{\alpha w}{2}\right)\right]^2 \int_{w/2}^{\infty} e^{-2\gamma(x-w/2)} dx \\ &\quad + \int_0^{w/2} [f(\alpha x)]^2 dx. \end{aligned} \tag{C1}$$

Here $f(x) = \cos x$ for even modes and $f(x) = \sin x$ for odd modes. For even modes,

$$\frac{1}{2}\int |\varphi|^2 dx = \frac{w}{4} + \frac{\sin\alpha w}{4\alpha} + \cos^2\frac{\alpha w}{2}\frac{1}{2\gamma}. \tag{C2}$$

Applying the characteristic equation $\tan\frac{\alpha w}{2} = \frac{\gamma}{\alpha}$, we have $\frac{\sin\frac{\alpha w}{2}\cos\frac{\alpha w}{2}}{2\alpha} = \frac{\sin^2\frac{\alpha w}{2}}{2\alpha\tan\frac{\alpha w}{2}} = \frac{\sin^2\frac{\alpha w}{2}}{2\gamma}$; then

$$\int |\varphi|^2 dx = \frac{w}{2} + \frac{1}{\gamma}. \tag{C3}$$

Following the same procedure, we obtain the same expression [Eq. (C3)] for odd modes.

2. Coupling coefficient

To calculate $m_{il}^{e(s)}$ and $g_{ij}^{e(s)}$ in Eq. (3), we should integrate the overlap between eigenmodes in different waveguides. Without loss of generality, we consider waveguide 1 with width w_1 centered at $x = 0$, and waveguide 2 with width w_2 centered at $(w_1 + w_2)/2 + d$; i.e., the gap between the waveguides is d. The effective mode index in waveguide 1 (2) is $n_{1(2)}$, and $\alpha_{1(2)} = k\sqrt{n_d^2 - n_{1(2)}^2}$, $\gamma_{1(2)} = k\sqrt{n_{1(2)}^2 - 1}$. The

coupling between waveguides 1 and 2 is

$$g_{12} = \frac{\left(n_d^2 - 1\right)k \int_{-w_1/2}^{w_1/2} f_1(\alpha_1 x) f_2\left(\frac{\alpha_2 w_2}{2}\right) e^{\gamma_2(x - w_1/2 - d)} dx}{2n_1\sqrt{\left(\frac{w_1}{2} + \frac{1}{\gamma_1}\right)\left(\frac{w_2}{2} + \frac{1}{\gamma_2}\right)}}, \tag{C4}$$

with $f_i(x) = \cos x$ ($\sin x$) for the even (odd) mode in the ith waveguide ($i = 1,2$). Since

$$\int_{-w_1/2}^{w_1/2} e^{i\alpha_1 x} e^{\gamma_2 x} dx = \frac{e^{(\gamma_2 + i\alpha_1)w_1/2} - e^{-(\gamma_2 + i\alpha_1)w_1/2}}{(\gamma_2 + i\alpha_1)}, \tag{C5}$$

we have

$$\int_{-w_1/2}^{w_1/2} f_i(\alpha_1 x) e^{\gamma_2 x} dx = f_i\left(\frac{\alpha_1 w_1}{2}\right) \frac{e^{\gamma_2 w_1/2}}{\gamma_2^2 + \alpha_1^2}[(\gamma_1 + \gamma_2) + e^{-\gamma_2 w_1}(\gamma_1 - \gamma_2)]. \tag{C6}$$

Therefore,

$$g_{12} = \frac{\left(n_d^2 - 1\right)k f_1\left(\frac{\alpha_1 w_1}{2}\right) f_2\left(\frac{\alpha_2 w_2}{2}\right)}{2n_1\sqrt{\left(\frac{w_1}{2} + \frac{1}{\gamma_1}\right)\left(\frac{w_2}{2} + \frac{1}{\gamma_2}\right)}} \times \frac{e^{-\gamma_2 d}[(\gamma_1 + \gamma_2) + e^{-\gamma_2 w_1}(\gamma_1 - \gamma_2)]}{\gamma_2^2 + \alpha_1^2}, \tag{C7}$$

and

$$g_{21} = \frac{\left(n_d^2 - 1\right)k f_1\left(\frac{\alpha_1 w_1}{2}\right) f_2\left(\frac{\alpha_2 w_2}{2}\right)}{2n_2\sqrt{\left(\frac{w_1}{2} + \frac{1}{\gamma_1}\right)\left(\frac{w_2}{2} + \frac{1}{\gamma_2}\right)}} \times \frac{e^{-\gamma_1 d}[(\gamma_1 + \gamma_2) + e^{-\gamma_1 w_2}(\gamma_2 - \gamma_1)]}{\gamma_1^2 + \alpha_2^2}. \tag{C8}$$

So, the effective coupling coefficient between the SW and EW is

$$g_{ij} = \sqrt{g_{ij}^s g_{ij}^e} = \frac{\left(n_d^2 - 1\right)k f_s\left(\frac{\alpha_s w_s}{2}\right) f_e\left(\frac{\alpha_e w_e}{2}\right)}{2\sqrt{\left(\frac{w_s}{2} + \frac{1}{\gamma_s}\right)\left(\frac{w_e}{2} + \frac{1}{\gamma_e}\right)}} \frac{1}{\sqrt{n_s n_e}} e^{-(\gamma_e + \gamma_s)d/2} \sqrt{\frac{[(\gamma_s + \gamma_e) + e^{-\gamma_e w_s}(\gamma_s - \gamma_e)][(\gamma_s + \gamma_e) + e^{-\gamma_s w_e}(\gamma_e - \gamma_s)]}{\left(\gamma_e^2 + \alpha_s^2\right)\left(\gamma_s^2 + \alpha_e^2\right)}}. \tag{C9}$$

APPENDIX D: APPROXIMATION FOR VERY LARGE ENVIRONMENT

1. Mode density

The characteristic equation for all eigenmodes in the waveguide can be written as

$$\left(\tan\frac{\alpha w}{2} - \frac{\gamma}{\alpha}\right)\left(\tan\frac{\alpha w}{2} - \frac{\alpha}{\gamma}\right) = 0. \tag{D1}$$

Since $\alpha = k\sqrt{n_d^2 - n_{\text{eff}}^2}$, $\gamma = k\sqrt{n_{\text{eff}}^2 - 1}$, then $\alpha^2 + \gamma^2 = (n_d^2 - 1)k^2$. This characteristic equation can be simplified as

$$\sin\alpha w = \frac{2\alpha\gamma}{\left(n_d^2 - 1\right)k^2}. \tag{D2}$$

When $w \gg \lambda$, the mode interval between two adjacent modes satisfies $\Delta\alpha \approx \pi/w$; i.e.,

$$\sqrt{n_d^2 - n_{\text{eff}}^2}k - \sqrt{n_d^2 - (n_{\text{eff}} + \delta)^2}k \approx \frac{\pi}{w}. \tag{D3}$$

Therefore, the mode index interval around n_{eff} is

$$\delta(n_{\text{eff}}) \approx \frac{\pi}{kw}\frac{\sqrt{n_d^2 - n_{\text{eff}}^2}}{n_{\text{eff}}}. \tag{D4}$$

Then, we obtain the mode density

$$\rho(n_{\text{eff}}) = \frac{1}{\delta(n_{\text{eff}})} = \frac{kw}{\pi}\frac{n_{\text{eff}}}{\sqrt{n_d^2 - n_{\text{eff}}^2}}. \tag{D5}$$

2. The normalized coupling coefficient

When $w_e \gg \lambda$, we can make the approximations

$$\frac{w_e}{2} + \frac{1}{\gamma_e} \approx \frac{w_e}{2}, \tag{D6}$$

$$e^{-\gamma_s w_e} \approx 0. \tag{D7}$$

Then the normalized coupling coefficient $g^2 w_e$ can be approximated by

$$g^2 w_e \approx A^2 B e^{-(\gamma_e + \gamma_s)d}, \tag{D8}$$

where

$$A = \frac{\left(n_d^2 - 1\right) f_s\left(\frac{\alpha_s w_s}{2}\right) f_e\left(\frac{\alpha_e w_e}{2}\right)}{\sqrt{w_s + \frac{2}{\gamma_s}}}\frac{1}{\sqrt{n_s n_e}}, \tag{D9}$$

$$B = \frac{\left(\sqrt{n_s^2 - 1} + \sqrt{n_e^2 - 1}\right)^2 + e^{-\gamma_e w_s}\left(n_s^2 - n_e^2\right)}{\left(n_d^2 - 1\right)^2 - \left(n_s^2 - n_e^2\right)^2}. \tag{D10}$$

As the characteristic function can also be written as

$$f\left(\frac{\alpha w}{2}\right)^2 = \frac{n_d^2 - n_{\text{eff}}^2}{n_d^2 - 1}, \tag{D11}$$

we finally obtain the normalized coupling coefficient for the large environment approximation,

$$g^2 w_e \approx \frac{\left(n_d^2 - n_s^2\right)\left(n_d^2 - n_e^2\right)}{n_s n_e\left(w_s + \frac{2}{\gamma_s}\right)} \times \frac{\left(\sqrt{n_s^2 - 1} + \sqrt{n_e^2 - 1}\right)^2 + e^{-\gamma_e w_s}\left(n_s^2 - n_e^2\right)}{\left(n_d^2 - 1\right)^2 - \left(n_s^2 - n_e^2\right)^2} \times e^{-(\gamma_e + \gamma_s)d}. \tag{D12}$$

3. Decay length

Under the near-resonant condition $n_e \approx n_s = n_0$, the normalized coupling coefficient becomes

$$g^2 w_e \approx \frac{k\left(n_d^2 - n_0^2\right)^2}{n_0^2\left(k w_s + \frac{2}{\sqrt{n_0^2-1}}\right)} \frac{4\left(n_0^2-1\right)}{\left(n_d^2-1\right)^2} e^{-2\sqrt{n_0^2-1}kd}. \quad \text{(D13)}$$

Substituting it into the spectrum density function [Eq. (9)], we have

$$J(n_0) \approx \frac{k\left(n_d^2 - n_0^2\right)^{3/2}}{n_0\left(k w_s + \frac{2}{\sqrt{n_0^2-1}}\right)} \frac{4\left(n_0^2-1\right)}{\left(n_d^2-1\right)^2} e^{-2\sqrt{n_0^2-1}kd}. \quad \text{(D14)}$$

From Eq. (7), the Dirac δ function $K(\tau) \approx J(n_0)\delta(\tau)$ leads to an exponential decay of energy in the system waveguide,

$$a(z) = e^{-J(n_0)z} = e^{-z/2L}. \quad \text{(D15)}$$

So, we can solve the decay length L for a mode in the SW with mode index n_0 as

$$L = \frac{1}{2J(n_0)} = \frac{1}{k} \frac{n_0\left(n_d^2-1\right)^2\left(k w_s + 2/\sqrt{n_0^2-1}\right)}{8\left(n_0^2-1\right)\left(n_d^2-n_0^2\right)^{3/2}} e^{2\sqrt{n_0^2-1}kd}. \quad \text{(D16)}$$

[1] H. P. Breuer and F. Petruccione, *The Theory of Open Quantum Systems* (Oxford University Press, New York, 2002).
[2] W. H. Zurek, Rev. Mod. Phys. **75**, 715 (2003).
[3] M. C. Fischer, B. Gutiérrez-Medina, and M. G. Raizen, Phys. Rev. Lett. **87**, 040402 (2001).
[4] K. Koshino and A. Shimizu, Phys. Rep. **412**, 191 (2005).
[5] B.-H. Liu, L. Li, Y.-F. Huang, C.-F. Li, G.-C. Guo, E.-M. Laine, H.-P. Breuer, and J. Piilo, Nat. Phys. **7**, 931 (2011).
[6] M. M. Wolf, J. Eisert, T. S. Cubitt, and J. I. Cirac, Phys. Rev. Lett. **101**, 150402 (2008).
[7] S. Diehl, A. Micheli, A. Kantian, B. Kraus, H. Büchler, and P. Zoller, Nat. Phys. **4**, 878 (2008).
[8] F. Verstraete, M. Wolf, and J. Cirac, Nat. Phys. **5**, 633 (2009).
[9] J. Barreiro, P. Schindler, O. Gühne, T. Monz, M. Chwalla, C. Roos, M. Hennrich, and R. Blatt, Nat. Phys. **6**, 943 (2010).
[10] H. Krauter, C. A. Muschik, K. Jensen, W. Wasilewski, J. M. Petersen, J. I. Cirac, and E. S. Polzik, Phys. Rev. Lett. **107**, 080503 (2011).
[11] L. Viola, E. Knill, and S. Lloyd, Phys. Rev. Lett. **82**, 2417 (1999).
[12] J. Du, X. Rong, N. Zhao, Y. Wang, J. Yang, and R. Liu, Nature (London) **461**, 1265 (2009).
[13] G. De Lange, Z. Wang, D. Riste, V. Dobrovitski, and R. Hanson, Science **330**, 60 (2010).
[14] I. Buluta and F. Nori, Science **326**, 108 (2009).
[15] I. Bloch, J. Dalibard, and S. Nascimbène, Nat. Phys. **8**, 267 (2012).
[16] A. Aspuru-Guzik and P. Walther, Nat. Phys. **8**, 285 (2012).
[17] R. Feynman, Int. J. Theor. Phys. **21**, 467 (1982).
[18] J. Barreiro, M. Müller, P. Schindler, D. Nigg, T. Monz, M. Chwalla, M. Hennrich, C. Roos, P. Zoller, and R. Blatt, Nature (London) **470**, 486 (2011).
[19] M. Hafezi, E. Demler, M. Lukin, and J. Taylor, Nat. Phys. **7**, 907 (2011).
[20] S. Longhi, Laser Photonics Rev. **3**, 243 (2009).
[21] I. Garanovich, S. Longhi, A. Sukhorukov, and Y. Kivshar, Phys. Rep. **518**, 1 (2012).
[22] X. Xiong, C.-L. Zou, X.-F. Ren, and G.-C. Guo, Opt. Express **21**, 17097 (2013).
[23] A. Yariv, *Quantum Electronics* (Wiley and Sons, New York, 1989).
[24] E. Hauge and J. Støvneng, Rev. Mod. Phys. **61**, 917 (1989).
[25] A. Snyder and J. Love, Appl. Opt. **15**, 236 (1976).
[26] M. Cai, O. Painter, and K. Vahala, Phys. Rev. Lett. **85**, 74 (2000).